Earth Planets Space, **63**, 335–349, 2011

A climatology study on ionospheric F_2 peak over Anyang, Korea

Eojin Kim[1], Jong-Kyun Chung[2], Yong Ha Kim[1], Geonhwa Jee[3], Sun-hak Hong[4], and Jeong-ho Cho[2]

[1]*Chungnam National University, Korea*
[2]*Korea Astronomy and Space Science Institute, Korea*
[3]*Korea Polar Research Institute, Korea*
[4]*Radio Research Agency, Korea Communication Commission, Korea*

(Received June 4, 2010; Revised March 2, 2011; Accepted March 30, 2011; Online published June 14, 2011)

We analyzed peak electron densities (N_mF_2) and peak heights (h_mF_2) of F_2 layer, measured by a digisonde at Anyang (37.4°N, 127.0°E, Geomag = 27.7°N, 196.9°E) during the period of April 1998 through April 2008. The Anyang N_mF_2 and h_mF_2 values averaged over each month show generally good linear relationship with increasing solar activities for all local time and for various geomagnetic activities. The change of the noon N_mF_2 with increasing solar flux indices ($F_{10.7}$) is much slower in summer than in other seasons, and the N_mF_2 difference between noon and midnight is minimized in summer. The h_mF_2 varies with $F_{10.7}$ from 200 km to 350 km at noon and from 300 to 450 km at midnight, but the h_mF_2 variations do not show seasonal difference significantly for all local time. The semi-annual variations of N_mF_2 and h_mF_2 are apparent and the winter anomaly of N_mF_2 is also clearly seen for most cases of geomagnetic and solar activities. The Anyang N_mF_2 values are in good agreement with the IRI 2007 model except for high solar and geomagnetic activity cases. However, the Anyang h_mF_2 values at midnight are significantly higher than the IRI model, being higher by up to ∼100 km for high solar activities.
Key words: N_mF_2, h_mF_2, ionosonde, mid-latitude ionosphere, climatology.

1. Introduction

The peak density of the F_2 layer (N_mF_2) and the height of the peak density (h_mF_2) from ionosondes have been studied as key parameters of ionospheric characteristics in various empirical models. These two parameters have also been used for time delay correction models of radio waves propagating through the Earth ionosphere. To correct the ionospheric time delay for single frequency GPS users, accurate calculation of the total electron content (TEC) between satellite and ground receiver is needed. In ionospheric time-delay algorithm developed by Klobuchar it is assumed that the constant phase of the diurnal variation of the time delay, proxy of N_mF_2, and the constant ionospheric height, proxy of h_mF_2 (Klobuchar, 1987). Because of varying characteristics of these parameters with the solar activities, seasons, locations, climatology analysis of N_mF_2 and h_mF_2 parameters measured in the GPS user region is needed to improve the time delay correction algorithm.

For the several decades, the N_mF_2 and h_mF_2 data obtained from the ionosonde stations have been investigated for the long term climatology of the ionosphere and the results of the various ionospheric model (CTIP, IRI) have been validated by the observed ionosonde data in the various conditions (Torr and Torr, 1973; Batista *et al.*, 1996; Bremer, 1998, 2004; Rishbeth *et al.*, 2000; Zou *et al.*, 2000; Richards, 2001; Sethi *et al.*, 2004, 2008; Liu *et al.*, 2006; Rishbeth, 2006; Oliver *et al.*, 2008). To investigate the variation of electron density distribution, they have considered the various effects of the solar activity and solar zenith angle, ionospheric dynamo, the global circulation from coupled thermosphere and ionosphere, tides from the lower atmosphere. Thanks to numerous investigations of the observed data, now it is well known that the solar activity, geomagnetic activity, season and local time are the key factors for the N_mF_2 and h_mF_2 variation. For example, Torr and Torr (1973) reported that the daytime N_mF_2 values in winter season are greater than in summer season in both hemispheres, known as the winter anomaly, and the N_mF_2 values are much higher in equinox seasons than solstice seasons at day and night time, known as semi-annual anomaly. In their paper, the seasons in which appearing maximum values of the noontime f_oF_2 (the proxy of N_mF_2) depend on the location for a given solar activity, hence the variation of the ionospheric parameters has different tendencies for different locations. The semi-annual and annual variations of h_mF_2 were reported by Rishbeth *et al.* (2000) using 16 ionosonde data. They also mentioned that although the h_mF_2 amplitudes of semi-annual variations increase with solar fluxes, the equinox maxima in h_mF_2 are related to thermospheric temperature variation probably due to tidal and wave inputs from the mesosphere and lower levels.

Semi-diurnal variations of the h_mF_2 for each season in the mid-latitude ionosphere were reported by Oliver *et al.* (2008) and Sethi *et al.* (2008). Kawamura *et al.* (2000) have published a climatology study of the winds and densities measured by a MU radar in Japan from 1986 to 1996. Analyzing drift velocity data from the MU radar, Oliver *et al.* (2008) suggested that the temporal variations of N_mF_2 and h_mF_2 are related to the changes of the density and temper-

doi:10.5047/eps.2011.03.011

Table 1. The total number of the digisonde data for the 9 combined cases.

	$F_{10.7} \leq 100$	$100 < F_{10.7} \leq 200$	$F_{10.7} > 200$
$K_p < 2$	(1) 10592	(2) 12359	(3) 2180
$2 \leq K_p < 4$	(4) 8097	(5) 18227	(6) 3273
$K_p \geq 4$	(7) 2323	(8) 7433	(9) 976

ature of neutral atmosphere as well as neutral wind variations.

The behaviors of the mid-latitude N_mF_2 and h_mF_2 are affected mainly by the solar activities, seasons and local times. The other causes such as a wind or geomagnetic activity seem to vary with geographic regions, suggesting that a comprehensive climatology analysis of the local ionosonde data is needed in order to establish an ionospheric correction model for GPS application in the region. To study the ionospheric climatology over Korea Peninsula, we utilized the N_mF_2 and h_mF_2 data from Anyang (37.4N, 127.0E) digisonde station. The digisonde data were sorted by the solar activities, geomagnetic activities, seasons and local times. Fitting parameter sets of N_mF_2 and h_mF_2 diurnal variations were derived for these various conditions. In addition, we compared the digisonde data with IRI-2007 model, the latest version of IRI model, and discuss the differences briefly. We also compared our results with those of Oliver *et al*. (2008) from a MU radar in Japan, and confirmed that the semi-diurnal variations of the h_mF_2 appeared for most seasons and semi-annual variations of the N_mF_2 are also apparent in our dataset.

2. Database and Analyzing Methods

The vertical ionospheric profiles used in this study were produced by two digital ionosonde systems, DGS-256 (April 1998–December 2004) and DPS-4D (November 2005–April 2008), at Anyang (37.4°N, 127.0°E, Geomag = 27.7°N, 196.9°E), operated by Korean Communications Commission (KCC). The vertical measurements of the sounding waves have been recorded every 60 minutes regularly with the accuracy of 1 kHz between 1 and 45 MHz and with a 10 km altitude bin in a 0–2560 km altitude range (Haines and Reinisch, 1995). The peak density of the ionospheric F_2 layer (N_mF_2) and the height of ionospheric peak density (h_mF_2) were scaled by an analysis tool, Automatic Real-Time Ionogram Scaling with True Height Analysis (ARTIST). DGS-256 had used the ARTIST version 4.0 and DPS-4D had used the ARTIST version 4.5.

The digisonde measurements of N_mF_2 and h_mF_2 span almost one cycle of solar activity, starting from 6 April 1998 to 5 April 2008 except for the period from 1 January to 27 November 2005 for the replacement of the instrument. The data period covers wide ranges of solar EUV flux proxy, $F_{10.7}$, from 65 to 298 solar flux units (sfu), and geomagnetic index, K_p index from 0 to 9, which are extensive enough to study ionospheric climatology over South Korea. We sorted the data for each geomagnetic or solar activity conditions and presented the N_mF_2 and h_mF_2 variations for the local times and seasonal conditions. To study the N_mF_2 and h_mF_2 variations for the seasons and local times and their responses to the solar and geomagnetic activities, we classified the data into 9 combined cases of solar and geomagnetic activities: (1) $K_p < 2$ & $F_{10.7} \leq 100$, (2) $K_p < 2$ & $100 < F_{10.7} \leq 200$, (3) $K_p < 2$ & $F_{10.7} > 200$, (4) $2 \leq K_p < 4$ & $F_{10.7} \leq 100$, (5) $2 \leq K_p < 4$ & $100 < F_{10.7} \leq 200$, (6) $2 \leq K_p < 4$ & $F_{10.7} > 200$, (7) $K_p \geq 4$ & $F_{10.7} \leq 100$, (8) $K_p \geq 4$ & $100 < F_{10.7} \leq 200$ and (9) $K_p \geq 4$ & $F_{10.7} > 200$. The numbers of the digisonde data (pairs of N_mF_2 and h_mF_2 at each hour) for the 9 combined cases are shown in Table 1. For the case 9, the number of data is relatively small.

There may be systematic differences of N_mF_2 and h_mF_2 due to the change of the digisonde and its analysis software. The Anyang data from DPS-4D with ARTIST 4.5 span November 28, 2005 through April 5, 2008, during which the solar activity was low, $F_{10.7}$ being less than 100 for 839 days among 851 observed days. Thus any systematic differences of N_mF_2 and h_mF_2 values due to the instrument change should be confined to the low solar activity cases.

3. Results

3.1 Solar activity variations

Previous studies have indicated that although variations of N_mF_2 and h_mF_2 are affected by geomagnetic activity (Rishbeth *et al*., 2000), their relation with geomagnetic activity seems complex (Bremer, 1998; Oliver *et al*., 2008), which is far from linear relation that is adopted in our current climatology analysis. Thus in this section we focus on N_mF_2 and h_mF_2 variations with the solar activities for given low, moderate, and high geomagnetic activity conditions.

Figure 1 shows N_mF_2 variations with $F_{10.7}$ for each low, moderate and high geomagnetic activity condition at midnight (0–1 LT) and at noon (12–13 LT) in January, April, July, and October. The Anyang data are indicated by circles at midnight and by triangles at noon. Solid and dashed lines are the linear fitting of the data, as

$$(N_mF_2 \text{ or } h_mF_2) = a(F_{10.7} - 100) + b \qquad (1)$$

where a is the mean slope of the responses of N_mF_2 or h_mF_2, b is the offset value of the fitting lines. The "+" and "×" symbols are the averaged IRI-2007 values at noon and midnight, respectively, within 12 bins of 25 solar flux unit (sfu) intervals from 0 to 300 sfu for the given conditions. The slopes of N_mF_2 variation with the solar activities (a) are 0.5, 5.7, 5.2, 2.4 ($\times 10^5$ el/cm^3) per 100 sfu unit at midnight and are changed to 8.7, 12.4, 1.9, 11.6 ($\times 10^5$ el/cm^3) per 100 sfu unit at noon for low geomagnetic activity condition in January, April, July, and October, respectively. The (b) values, the fitting values at $F_{10.7} = 100$, are 1.2, 3.5, 3.8, 2.2 ($\times 10^5$ el/cm^3) at midnight and increase to 6.3, 9.6, 7.2, 9.1 ($\times 10^5$ el/cm^3) at noon for the corresponding months.

In equinoctial months (April, October), the noon time N_mF_2 values are in the range of 3–28$\times 10^5$ electron/cm^3,

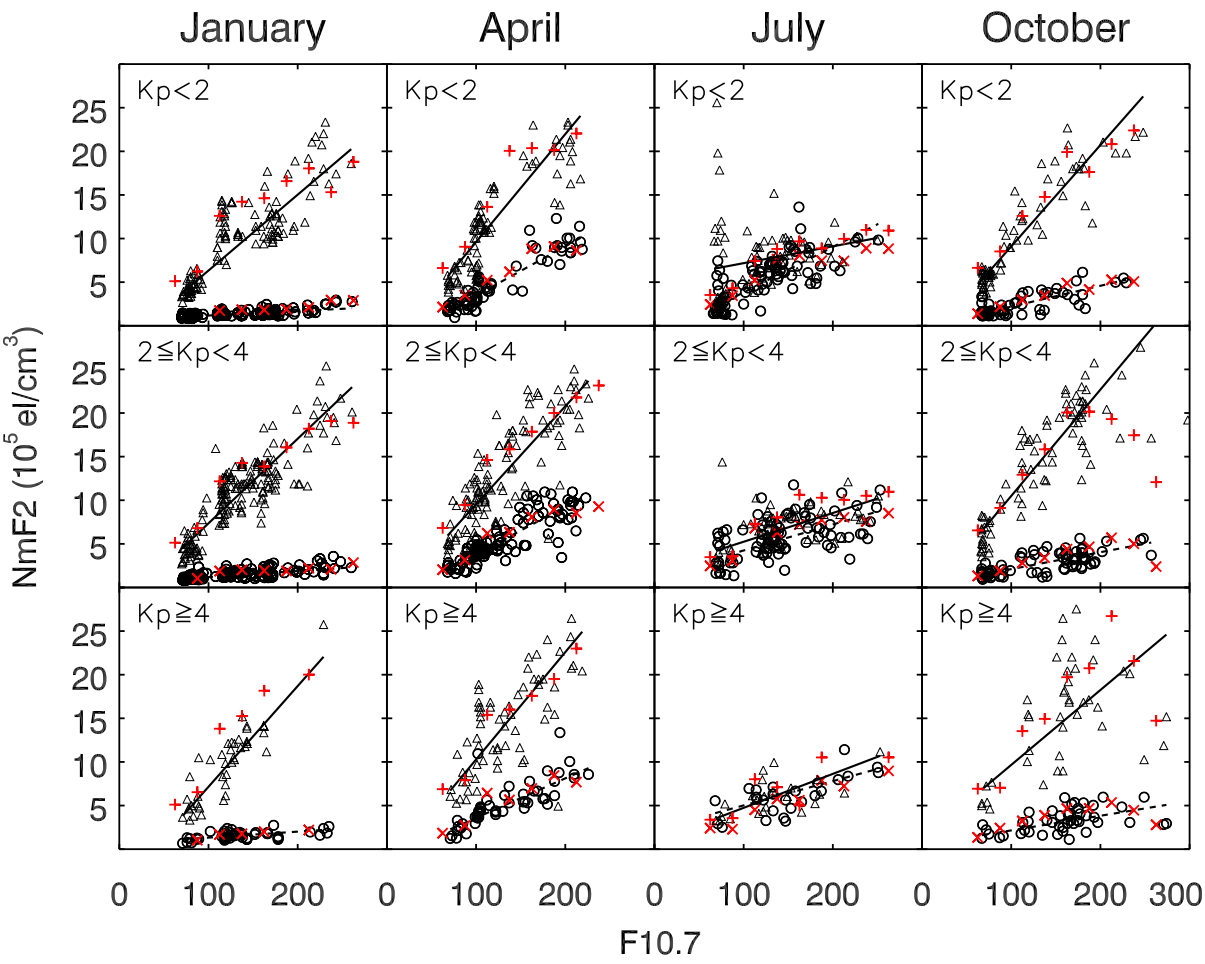

Fig. 1. The N_mF_2 variation with solar activity for low, moderate and high geomagnetic conditions in January, April, July and October at midnight (0–1 LT) (circle) and at noon (12–13 LT) (triangle). Solid and dashed lines are the linear fitting of the digisonde data at noon and at midnight. The "+" and "×" symbols are averaged N_mF_2 values of the IRI-2007 model at noon and midnight for the corresponding cases, respectively.

increasing with $F_{10.7}$ in the quiet and moderate geomagnetic activity condition, and N_mF_2 at midnight is less than 13×10^5 electron/cm^3. The difference of the N_mF_2 between noon and midnight is getting higher with increasing solar activity. The patterns of the N_mF_2 variation for each geomagnetic activity conditions are very similar in winter month (January) and equinoctial months (April, October), except that the N_mF_2 difference between noon and midnight is higher in winter than in other seasons, probably due to recombination during longer time after sunset. On the other hand, the pattern of N_mF_2 in summer (July) is quite different from other seasons. Most N_mF_2 values in July are less than 10×10^5 el/cm^3 even in high solar activity and the response of N_mF_2 is very similar at noon and at midnight, resulting in only small N_mF_2 difference between noon and midnight even in high solar activity. The N_mF_2 responses with $F_{10.7}$ in January, and in July are consistent with those reported by Bremer (1998). Correlation coefficients at noontime for low geomagnetic activity condition are more than 0.86 for all months except summer months, when the data are scattered severely for $K_p < 2$. We will discuss causes of the scattered N_mF_2 values during summer in later sections. Overall, Fig. 1 shows that the Anyang N_mF_2 data are consistent with the IRI-2007 values for all seasons and solar activities.

The variation of h_mF_2 also shows the good linear relationship with $F_{10.7}$. In Fig. 2, the h_mF_2 values are mainly distributed from 300 to 450 km at midnight, and from 200 to 350 km at noon for all conditions, even for the high geomagnetic activity. The slopes of h_mF_2 variation with the $F_{10.7}$ (a) are 37, 43, 76, 36 km per 100 sfu at midnight and are enhanced to 57, 73, 94, 64 km per 100 sfu at noon for low geomagnetic activity condition in January, April, July, and October, respectively. The offset values (b) are 323, 328, 325, 314 km at midnight and decrease to 230, 261, 234, 243 km at noon for the corresponding months. The exact values of fitting parameters are affected by the Anyang data obtained from the different digisonde during the period of 2005–2008, although they were mainly for low solar activities. The correlations between noon h_mF_2 values and $F_{10.7}$ indices are very clear with coefficients larger than 0.76 for low geomagnetic conditions, but the correlations are degraded for high geomagnetic activities. The h_mF_2 variation with solar activities shows very little change with season, contrary to that of N_mF_2, which has been noted by Bremer (1998). The IRI-2007 values of h_mF_2, however, show significant discrepancies from the Anyang data, especially at midnight in high solar flux indices and high geomagnetic cases. The IRI-2007 values seem to increase but quickly be saturated with $F_{10.7}$, resulting in up to ~100 km lower val-

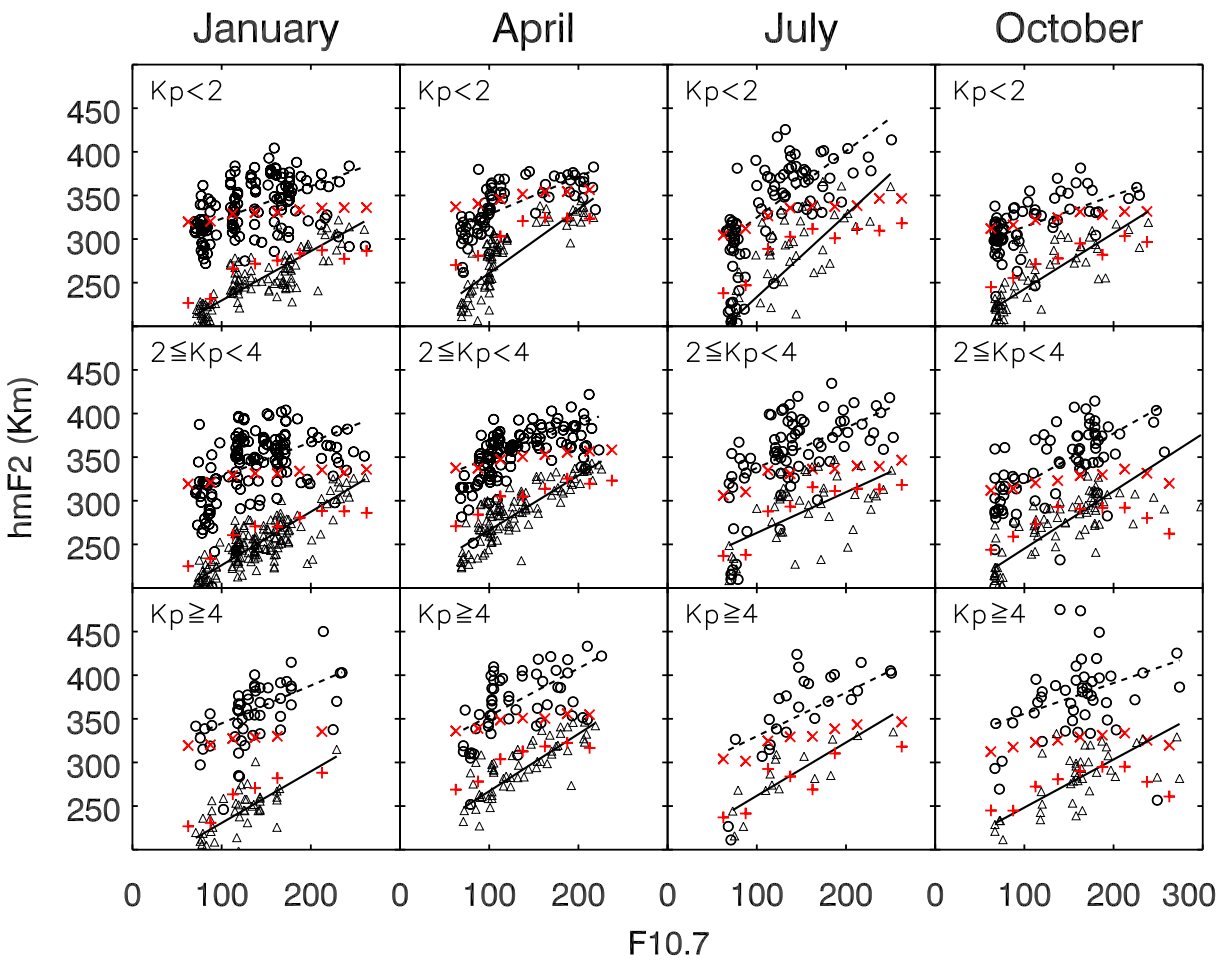

Fig. 2. The h_mF_2 variation with solar activity for low, moderate and high geomagnetic conditions in January, April, July and October at midnight (0–1 LT) (circle) and at noon (12–13 LT) (triangle). The "+" and "×" symbols are averaged h_mF_2 values of the IRI-2007 model at noon and midnight for the corresponding cases, respectively.

ues than the Anyang h_mF_2 values. The h_mF_2 discrepancies are perhaps the most critical aspect if the IRI-2007 model is used for GPS applications in North East Asia, or at least over Korean peninsula.

The variation of N_mF_2 values and h_mF_2 values with the solar activity may be different for increasing and decreasing phases, as previous studies have shown (Huang and Cheng, 1996; Triskova and Chum, 1996; Bremer, 2001; Adler and Elias, 2008). We note that both N_mF_2 and h_mF_2 seem to have different slopes with $F_{10.7}$ for increasing and decreasing phases, but we don't have enough data, especially for the increasing phase, to separate clearly the hysteresis. The linear fitting for the change with $F_{10.7}$ in Eq. (1) is not meant to contrast with the IRI model which shows saturation trend at high solar activity, but meant to make a simple climatology model that can provide with quick ionospheric correction for GPS used in Korea. Our data are spread widely, burying the saturation trend for high $F_{10.7}$'s, but still clearly show significant h_mF_2 difference from the IRI model. Oliver *et al.* (2008) noted small reduction of the slope in F_2 peak altitudes vs $F_{10.7}$, but they too make a linear fitting for their climatology model over Japan.

3.2 Seasonal variations

To study the seasonal variations of the N_mF_2 and h_mF_2, we averaged the Anyang data of each month at noon (triangles) and midnight (circles) for the nine cases of combined solar and geomagnetic conditions, as presented in Figs. 3 and 4. The standard deviations from the averaged values are shown with error bars in the figures, which also show IRI-model values at noon ("+" symbols) and at midnight ("×" symbols) for comparison. We fitted data at noon (solid line) and at midnight (dashed line) by the harmonic function which contains annual and semi-annual components, as follows.

$$f = a_0 + a_1 \cos\left[\frac{2\pi}{P_1}(t - a_2)\right] + a_3 \cos\left[\frac{2\pi}{P_2}(t - a_4)\right] \quad (2)$$

In this function, a_0 is the mean value of the data and a_1, a_3, a_2, a_4 indicate the amplitudes and the phases of the annual and semi-annual variations, respectively. P_1 and P_2 are 12 and 6 months, the periods of annual and semi-annual variation, respectively, and t is a month.

In Fig. 3, it seems evident for all case except one case (high solar and geomagnetic activity condition) that noon N_mF_2 values show apparent semi-annual variation, whereas midnight N_mF_2 values do dominant annual variation. Specifically, two maxima of noon N_mF_2 values appear around April and October, representing the semi-annual anomaly which is the typical characteristic of mid-latitude ionosphere. The maximum of midnight N_mF_2 values oc-

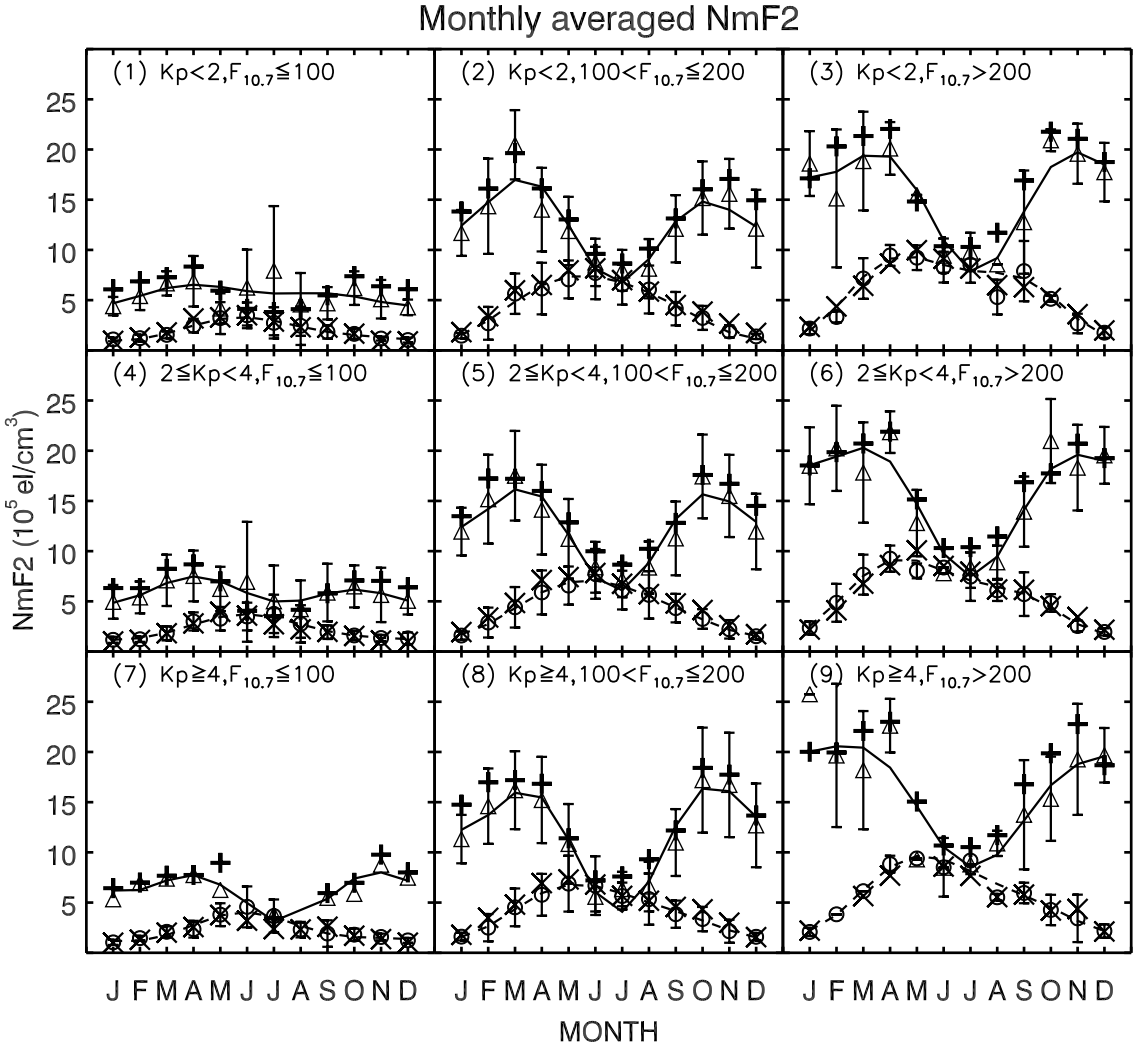

Fig. 3. Monthly averaged N_mF_2 measured by the Anyang digisonde at midnight (circle) and noon (triangle) with error bars. The harmonic function fittings of monthly averaged N_mF_2 values are shown with dashed and solid lines for midnight and noon times, respectively. The averaged IRI-2007 N_mF_2 values are overlapped with "×" and "+" symbols for midnight and noon times, respectively.

curs around June for low solar activities, but for higher solar activity cases it appears in earlier months. In contrast, noon N_mF_2 values show an annual minimum during summer months, approximately opposite to midnight N_mF_2 values, especially for high solar activity cases. The case of high geomagnetic and high solar activity condition (Fig. 3(9)) does not have enough data points to be judged. The noon N_mF_2 values are much higher in winter than summer, and this characteristic is more significant for higher solar activities, which is known as winter anomaly. Monthly averaged IRI-2007 N_mF_2 values at midnight ("×" symbols) shows better agreements with the Anyang data than their noon values ("+" symbols) for all cases. Due to the absence of the ion production by solar EUV radiation after sunset, midnight N_mF_2 values are lower than noon N_mF_2 values by more than 5×10^5 el/cm^3 for low solar activity, 10×10^5 el/cm^3 for moderate and high solar activity conditions except in summer months. Especially in January and December, midnight N_mF_2s are almost the same for all cases of solar and geomagnetic activities. However, in summer months (May, June, July, August), especially in July, the differences between noon and midnight N_mF_2 values are very small or reversed in some cases. Note that the noon N_mF_2 values in summer decrease with increasing geomagnetic activities. Moreover, in the case of the high geomagnetic and moderate solar activity, the midnight N_mF_2 in July is higher than the noon N_mF_2, which may indicate the effect of the negative ionospheric storm during the disturbed period.

In Fig. 4, both noon and midnight h_mF_2 values show semi-annual variation for low and moderate solar activity cases, but annual variation is clear for high solar activity cases. Both noon and midnight h_mF_2 values are higher for high solar activity than for low solar activity, but they do not show significant difference for geomagnetic activities. The annually averaged noon h_mF_2 values are 229, 289, and 311 km for low, moderate and high solar activity cases respectively, and their monthly variations from the annual averages are as large as 17 km for each case. Both noon and midnight h_mF_2 values of the IRI model are within statistical spread bars of the Anyang data for the cases of low solar activity ($F_{10.7} \leq 100$), although the IRI values tend to distributed close to the high end of the bars. Note that the Anyang data for low solar activity include data obtained from ARTIST version 4.5, which may affect the comparison

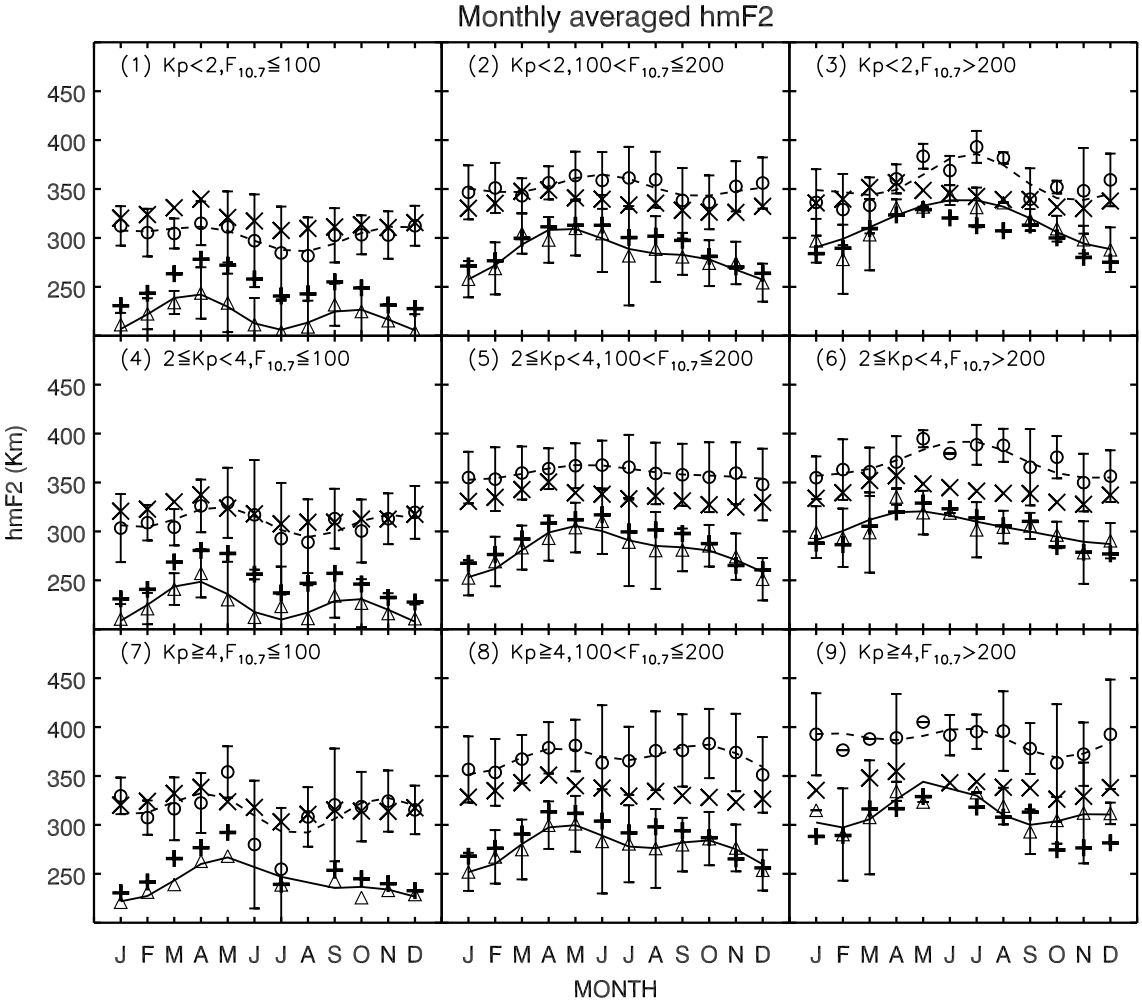

Fig. 4. Monthly averaged h_mF_2. The symbols are the same as in Fig. 3.

with the IRI model. For the higher solar activity the Anyang h_mF_2 values at midnight are persistently higher than the IRI model, while the noon h_mF_2 values are in good agreement with IRI model. The discrepancy seems to increase with increasing K_p, although there are not enough data to be compared with for the case of high geomagnetic and high solar activity condition. Note that the Anyang h_mF_2 values at midnight for the high solar activity show a maximum in summer months, departing more from the IRI values than other months. Accordingly, the fact that the measured h_mF_2 values at midnight are higher than the IRI model especially for high solar activity should be considered seriously when the IRI model is utilized in the mid-latitude region or at least in the Korean peninsula. Furthermore, the IRI model h_mF_2 values at midnight seem to be almost immune to solar activity and be of little monthly variation, which differs significantly from reality.

3.3 Local time variation

The variations of Anyang N_mF_2 and h_mF_2 values with local time are presented in Figs. 5, 6 and Figs. 7, 8, respectively. Circles with error bar indicate the Anyang data averaged in 1 hour bins and "×" symbols are the IRI model. The solid curved lines indicate the least square fitting of Anyang N_mF_2 and h_mF_2 values with the harmonic function of Eq. (2) for daily variations.

In Figs. 5 and 6, the changes of the N_mF_2 values are dominated by the diurnal variation for all seasons, and maximum N_mF_2 values increase with the solar activity except in July. In July, the representative month of summer, dependency of N_mF_2 values on the solar activity is drastically reduced. Note that the N_mF_2 patterns of low solar activity cases in July are significantly different from higher solar activity cases and their error bars are unusually large because sudden enhancements of N_mF_2 during daytime occurred frequently in summer for the quiet period from 2006 to 2007, which will be discussed in Section 4. In most cases, the N_mF_2 is minimized around 5 LT just before sunrise, and it rapidly increases after sunrise, obviously due to ionization by solar EUV flux. Dependency of geomagnetic activity on the N_mF_2 values is not clear, although the maximum N_mF_2 increases with geomagnetic activity in some cases. The maximum N_mF_2 appears around 12 LT for all geomagnetic and solar activities in January and October, whereas the maximum is delayed by as much as 2–3 hours for the cases of low and moderate solar activity in April. In July, N_mF_2 variations are too small to determine the maximum time reliably. In January, N_mF_2 show particularly small error bars for all cases, compared to other seasons. Note that the error bars are sometimes omitted in the figure where reliable fitting cannot be made due to lack of data, especially

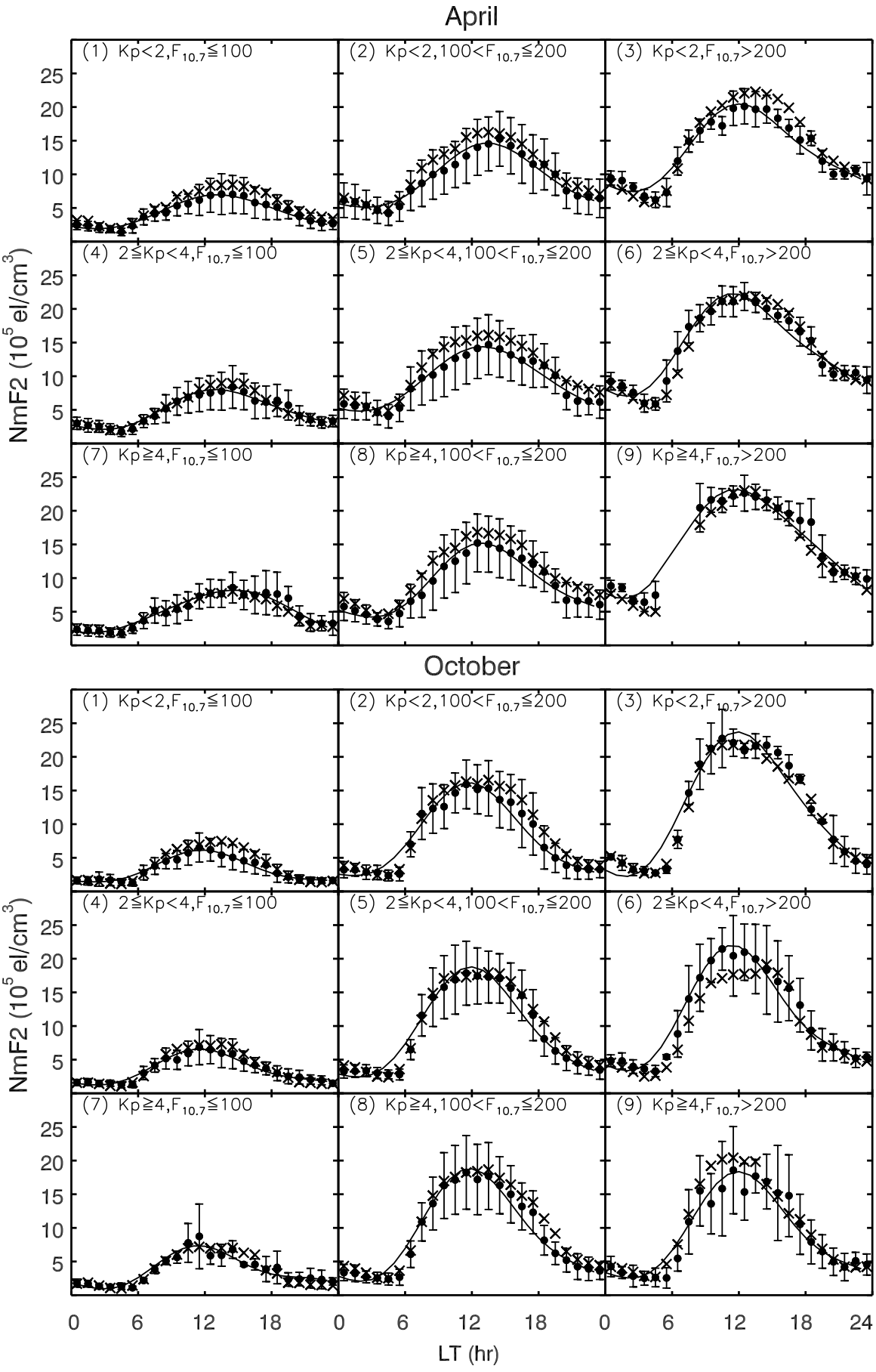

Fig. 5. Hourly averaged N_mF_2 values versus local times in April and October for the 9 combined cases. The Anyang and IRI-2007 model N_mF_2 values are shown with filled circles with error bar and "×" symbols, respectively. Solid lines indicate the fitting of the averaged Anyang N_mF_2 values.

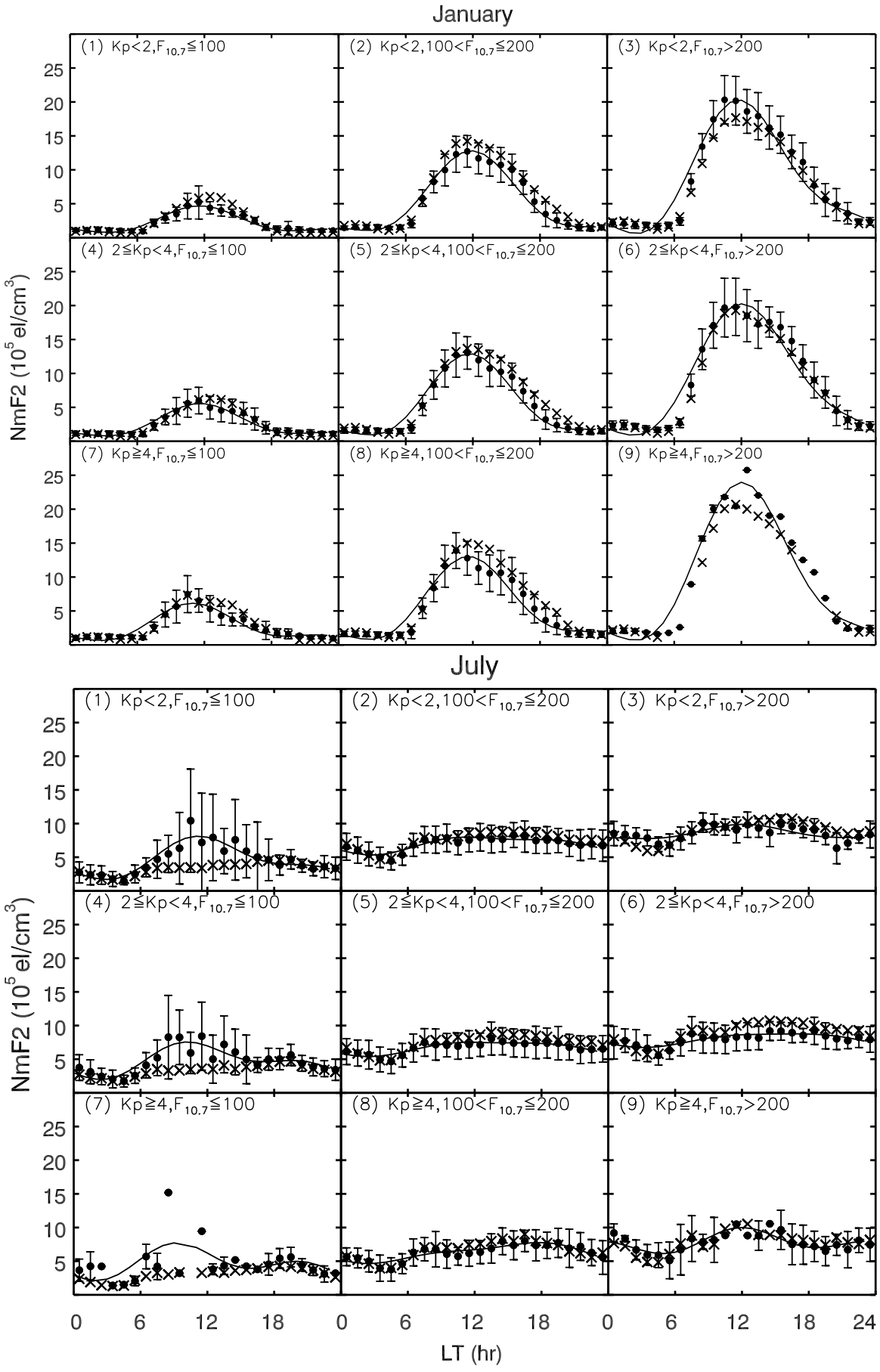

Fig. 6. Hourly averaged N_mF_2 values versus local times in January and July for the 9 combined cases. The symbols are the same as in Fig. 5.

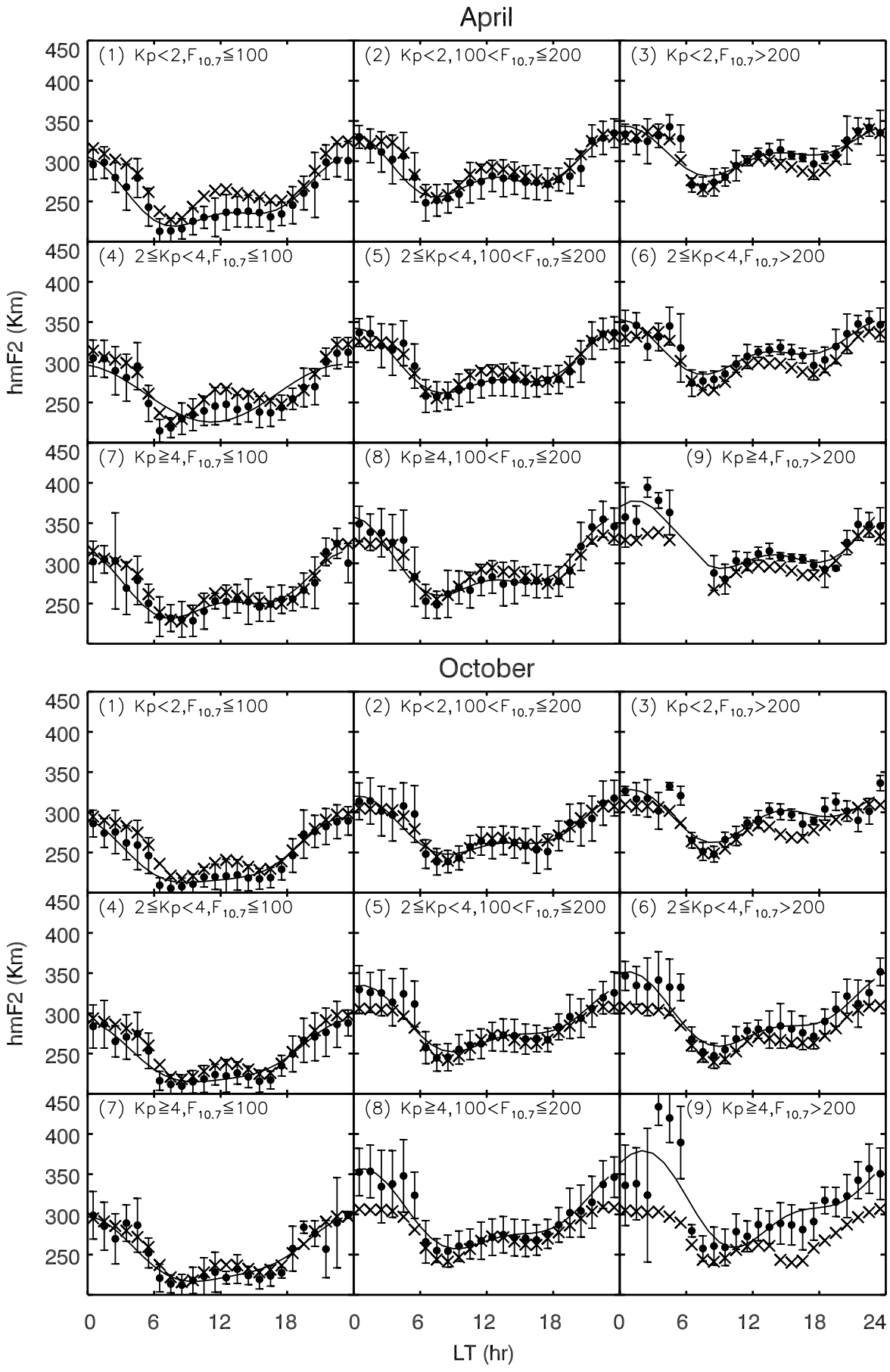

Fig. 7. Hourly averaged h_mF_2 values versus local times in April and October for the 9 combined cases. The symbols are the same as in Fig. 5.

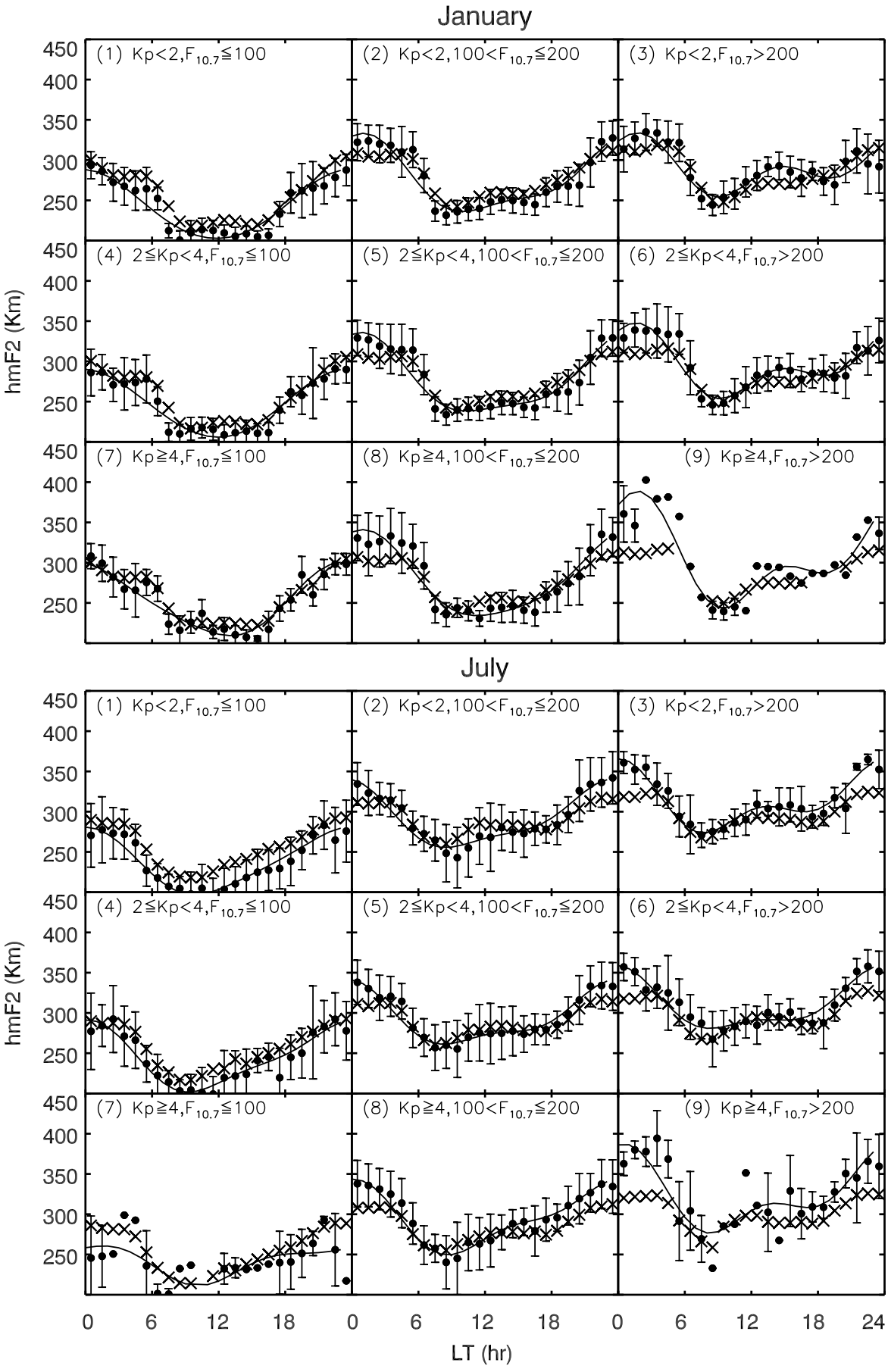

Fig. 8. Hourly averaged $h_m F_2$ values versus local times in January and July for the 9 combined cases. The symbols are the same as in Fig. 5.

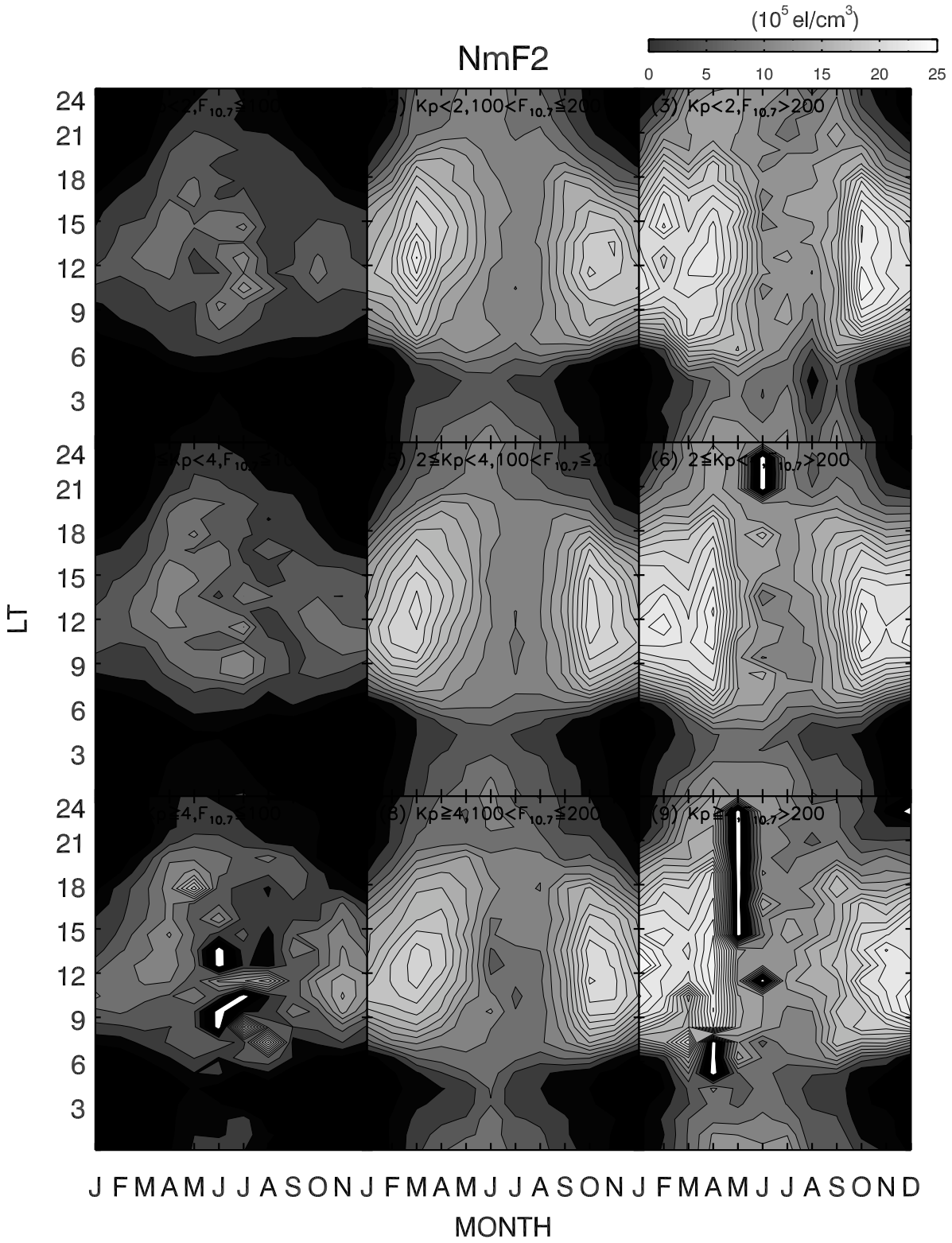

Fig. 9. Monthly and local time variations of the Anyang N_mF_2 values during the period of 1998–2008. The left, center, right panels are for low, medium, high geomagnetic activity conditions, respectively. The upper, middle, and lower panels are for low, medium, high solar activity conditions, respectively.

for some cases of the high geomagnetic condition. The IRI-2007 model well traces the Anyang N_mF_2 values for most cases with noticeable departure for the cases of low solar activity in July. We will discuss this departure in the next section.

In Figs. 7 and 8, h_mF_2 variations with local time seem to follow a general pattern: low during daytime, high at night. The lowest value of h_mF_2 increases with increasing solar activity, namely, 210 km, 259 km, and 282 km for low, moderate and high solar activity, respectively. The highest value of h_mF_2 values also seems to increase with solar activities, which is not predicted in the IRI model that

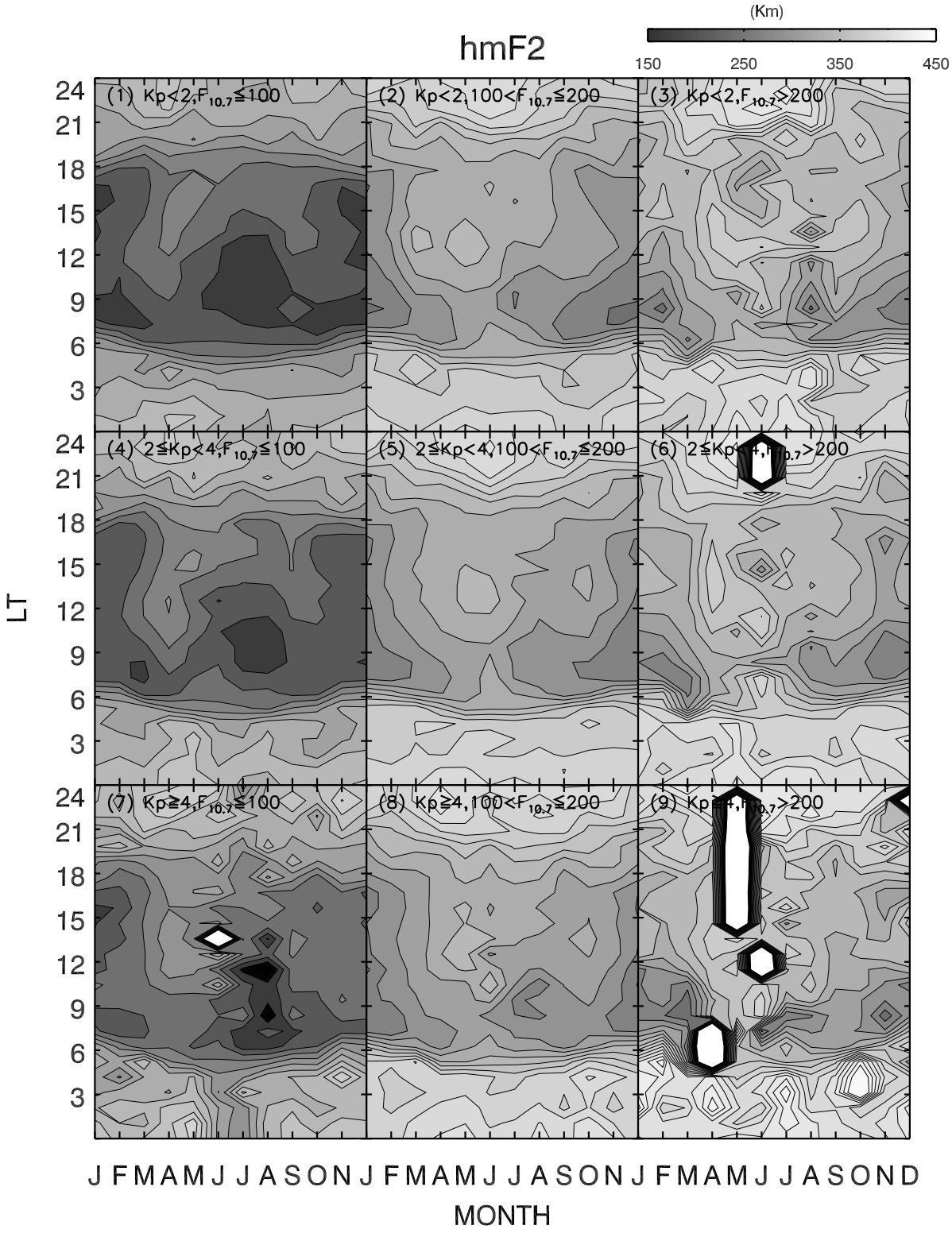

Fig. 10. Monthly and local time variations of the Anyang $h_{\mathrm{m}}F_2$ values during the period of 1998–2008. Panels are arranged same as in Fig. 9.

shows the almost same value at midnight regardless solar activity. Overall the IRI model tends to give higher and lower altitudes than the Anyang $h_{\mathrm{m}}F_2$ values for low and high solar activities, respectively. Note that the Anyang $h_{\mathrm{m}}F_2$ values for the low solar activity case may have been affected by the instrument change in 2005. However, the Anyang $h_{\mathrm{m}}F_2$ values at midnight are clearly higher than the IRI model for high solar activity and for moderate solar activity for some months as well. These features were noted in Fig. 2, implying that the IRI model $h_{\mathrm{m}}F_2$ values may not be a good parameter to be used in GPS correction algorithms, especially for high solar activity condition in mid-latitude or at least over Korean peninsula. Accurate estimates of $h_{\mathrm{m}}F_2$ values are particularly important for GPS correction procedures because they are regarded as pierce point altitudes along GPS signal path from GPS satellites to

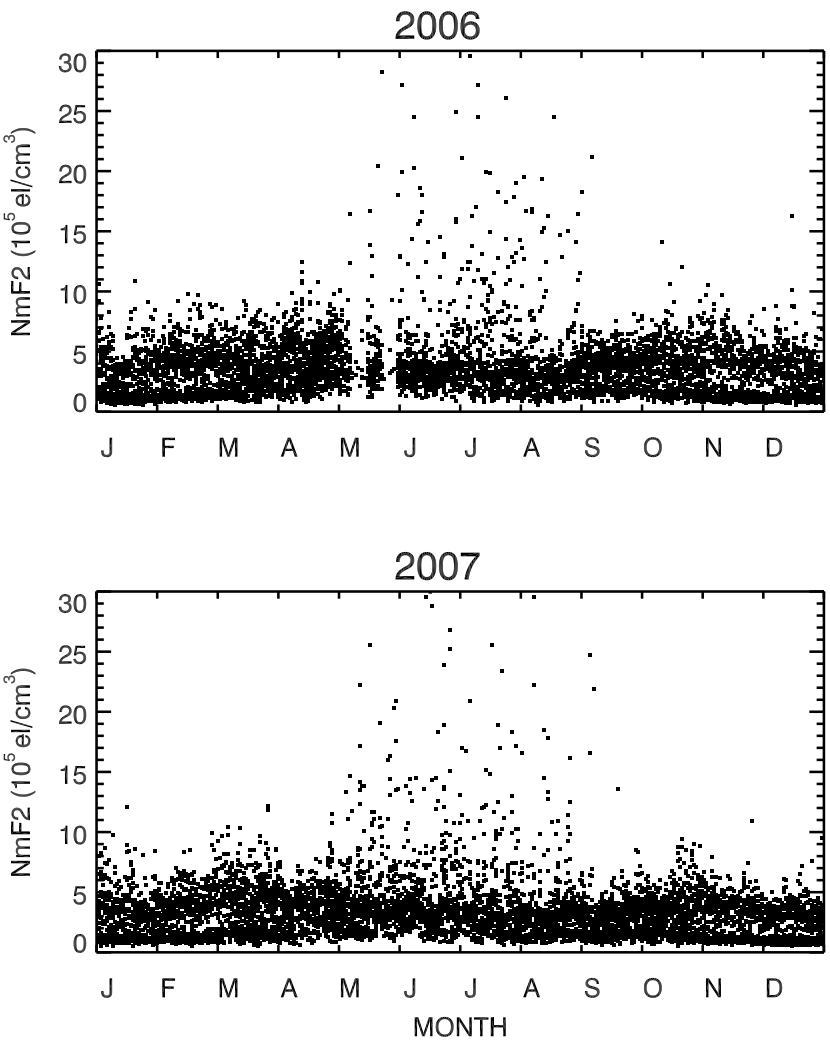

Fig. 11. Anyang digisonde N_mF_2 values observed in 2006 and 2007.

a GPS receiver on the ground.

Figures 9 and 10 show variations of monthly averaged N_mF_2 and h_mF_2, respectively, with both local time and month. In Fig. 9, daytime N_mF_2 values show clear semi-annual variation for moderate and high solar activity cases. In addition, winter N_mF_2 values are noticeably larger than summer values especially for high solar activity cases, confirming the winter anomaly as reported at other mid-latitude stations. For the medium solar activity cases, the differences of noontime N_mF_2 values between summer and other season are intensified as the geomagnetic activity increases. For the high geomagnetic and medium solar activity case (lower and middle panel), the peak N_mF_2 is shifted toward afternoon in the vernal equinox season. Two other high geomagnetic cases (lower left and lower right panels) have rather noisy contours due to shortage of data. The varying magnitudes of the N_mF_2 with both local time and season increase with both increasing solar and geomagnetic activities, as shown in Figs. 5 and 6. In Fig. 10, the h_mF_2 variations with local time show a maximum at midnight and minimum at pre-noon or post-noon except two cases (lower left and lower right panels). Unlike N_mF_2, the h_mF_2 variations are not dominated by semi-annual components.

4. Discussions

Although actual patterns of N_mF_2 seasonal variations are different over the globe as reported by Torr and Torr (1973), it is well known that semi-annual variation and the winter anomaly of N_mF_2 are typical characteristics in the mid-latitude ionosphere. Our results generally confirmed these characteristics, but the semi-annual variation and the winter anomaly are not very significant for low solar activity cases. In addition, our data show little response of the N_mF_2 to the geomagnetic activity, probably since Anyang station is located at the relatively low geomagnetic latitude (27.7°N). Oliver *et al.* (2008) interpreted the insensitivity to the geomagnetic activity as compensation among the processes that affect F-region electron densities.

The Anyang data are generally consistent with the IRI-2007 model for most cases. However, the most significant difference between the Anyang data and the IRI-2007 model is the behaviors of h_mF_2 values. Anyang h_mF_2 values vary linearly with $F_{10.7}$, whereas the IRI h_mF_2 values show little dependency on $F_{10.7}$, resulting in significant differences from the Anyang data for high solar activities, as shown in Fig. 2. In Fig. 4, monthly averaged IRI h_mF_2 values at midnight are lower, although some are within the standard deviation bars of our data, than the corresponding

values of the Anyang h_mF_2, when $F_{10.7}$ is greater than 100. In Figs. 7 and 8, the IRI h_mF_2 values are lower than the Anyang data during night time for the moderate and high solar activity cases, and even during daytime for the high solar activity case. This analysis of our h_mF_2 values for the moderate and high solar activity cases should not be affected by any systematic differences that might have been caused by the instrument change in 2005, because since then the solar activity was predominantly low, $F_{10.7}$ being less than 100 for almost all the observed days, as pointed out in Section 2.

The variations of our h_mF_2 values with solar activities (Fig. 2), seasons (Fig. 4), and local times (Figs. 7 and 8) are consistent with Kawamura *et al.* (2000)'s climatology study on the F layer measured by a MU radar in Japan. We also compared our h_mF_2 values with those from Kokubunji, Japan and from Juliusruh, German in the format of Fig. 2, and found overall consistency with them.

According to Oliver *et al.* (2008) that interpreted Kawamura *et al.* (2000)'s data, the F_2 peak altitude increases with solar activities since thermal expansion of thermosphere due to increased solar EUV raises the altitude where the chemistry and diffusion processes are balanced. Namely, chemical recombination is more effective by the increased neutral molecular densities and diffusion is less effective by the increased neutral atomic densities as solar activity increases. Oliver *et al.* (2008) also shows that both seasonal and diurnal variations of the F_2 peak altitude are strongly controlled by neutral winds which were measured by a MU radar simultaneously with F_2 peak densities and altitudes. Equatorward (poleward) meridional winds can raise (lower) the ionization to where the neutral molecular densities are low (high) and thus the chemistry-diffusion balance height is changed. They noted very low F_2 peak on winter mornings at solar minimum and very high on summer nights at solar maximum, which can be confirmed in Figs. 7 and 8. They also pointed out that at solar minimum the midnight level of the F_2 peak is almost independent of season, while the midday level depends strongly on season, which is also consistent with Fig. 4. Therefore, our analysis of the Anyang data seems practically representative at the mid-latitude, or over at least Korean peninsula, despite the significant discrepancy of h_mF_2 values from the IRI-2007 model.

As pointed out previously, the daytime Anyang N_mF_2 values in July for low solar activity cases are significantly larger than the IRI-2007 model with big error bars. This is due to the fact that the sudden enhancements of the daytime N_mF_2 appear in summer months (May $\sim$ August) for the low solar activity periods from 2006 to 2007 as shown in Fig. 11. For more than 12% of total daytime data, the Anyang N_mF_2 values increase to 30×10^5 el/cm^3 suddenly and decrease in one hour. The average N_mF_2 except these enhanced values during daytime (08–18 LT) is about 4×10^5 el/cm^3, which is close to the corresponding IRI values. These enhancements affect hourly averaged values and cause large error bar as shown in Fig. 6 during daytime for the low solar activity cases. However, the sudden enhancements did not occur during the period from 1998 to 2004, during which solar activity was high and summer N_mF_2 values at day and night were lower than those in winter and equinox seasons. The sudden enhancements in our N_mF_2 data seem to have similar characteristics of N_mF_2 quiet time disturbances studied by Mikhailov *et al.* (2009), but further careful analysis of this part of data is needed.

5. Summary

To study the climatology of the mid-latitude ionosphere over Korean Peninsula, we analyzed the ionosonde N_mF_2 and h_mF_2 data measured at Anyang station during the period of 1998–2008 and compared them with model values of IRI-2007. The variations of N_mF_2 values and h_mF_2 values with the solar activities, seasons, and local times were investigated for the 9 combined cases of solar and geomagnetic activities. When the N_mF_2 data were sorted in seasonal and local time bins, correlations of N_mF_2 values with the solar activities are apparent for low and moderate geomagnetic activities. The responses of noon N_mF_2 values to the solar activity are higher in January than in July, while the solar activity responses of h_mF_2 do not show the significant differences over seasons. Those responses are little dependent on geomagnetic activities. Both monthly averaged N_mF_2 values and h_mF_2 values show clear semi-annual variations at noon and annual variations at midnight. Noontime N_mF_2 values are larger in winter than summer, confirming the winter anomaly. Magnitudes of N_mF_2 local time variation increase with increasing solar activities except in July when the local time variation is barely seen. The Anyang h_mF_2 decreases rapidly at sunrise during all seasons, and shows marginal semidiurnal variation. The IRI-2007 model N_mF_2 values are mostly consistent with the Anyang data, but the model h_mF_2 values at midnight are significantly lower than the Anyang data, especially for high solar activities. This h_mF_2 discrepancy should be recognized when IRI model is updated for mid-latitude regions. Parameterized results of our climatology analysis may significantly contribute to improving GPS correction algorithms used in Korean peninsula, particularly because accurate estimates of h_mF_2 as ionospheric pierce points of GPS signal paths are important for GPS correction procedures.

Acknowledgments. We thank for the support by BK 21 Advanced Research and Education for Astronomy and Space Observations and this work partially supported by Space Geodesy group, Korea Astronomy and Space Science Institute, Korea. We also thank Space Weather Division, Icheon Branch of Radio Research Agency, Korea Communication Commission (KCC), Korea, providing Anyang digisonde data.

References

Adler, de N. O. and A. G. Elias, Latitudinal variation of *fo*F2 hysteresis of solar cycles 20, 21 and 22 and its application to the analysis of long-term trends, *Ann. Geophys.*, **26**, 1269–1273, 2008.

Batista, I. S., M. A. Abdu, R. T. de Medeiros, and E. R. de Paula, Comparison between IRI predictions and digisonde measurements at low latitude station, *Adv. Space Res.*, **18**, 49–52, 1996.

Bremer, J., Trends in the ionospheric E and F regions over Europe, *Ann. Geophys.*, **16**, 986–996, 1998.

Bremer, J., Trends in the thermosphere derived from global ionosonde observations, *Adv. Space Res.*, **28**, 997–1006, 2001.

Bremer, J., Investigations of long-term trends in the ionosphere with worldwide ionosonde observations, *Adv. Radio Sci.*, **2**, 253–258, 2004.

Haines, D. M. and B. W. Reinisch, *Digisonde Portable Sounder System Manual*, 2 pp., University of Massachusetts Lowell Center for Atmo-

sphere Research, 1995.

Huang, Y.-N. and K. Cheng, Solar cycle variations of the equatorial ionospheric anomaly in total electron content in the Asian region, *J. Geophys. Res.*, **101**, 24513–24520, 1996.

Kawamura, S., Y. Otsuka, S.-R. Zhang, and S. Fukao, A climatology of middle and upper atmosphere radar observations of thermospheric winds, *J. Geophys. Res.*, **105**, 12777–2788, 2000.

Klobuchar, J. A., Ionospheric time-delay algorithm for single-frequency GPS users, *IEEE Transactions on Aerospace and Electronic Systems*, AES-23, 325–331, 1987.

Liu, L., W. Wan, and B. Ning, A study of the ionogram derived effective scale height around the ionospheric hmF2, *Ann. Geophys.*, **24**, 851–860, 2006.

Mikhailov, A. V., A. H. Depueva, and V. H. Depuev, Quiet time F2-layer disturbances: seasonal variations of the occurrence in the daytime sector, *Ann. Geophys.*, **27**, 329–337, 2009.

Oliver, W. L., S. Kawamura, and S. Fukao, The causes of mid-latitude F layer behavior, *J. Geophys. Res.*, **113**, 8310–8323, 2008.

Richards, P. G., Seasonal and solar cycle variations of the ionospheric peak electron density: Comparison of measurement and models, *J. Geophys. Res.*, **106**, 12803–12819, 2001.

Rishbeth, H., F-region links with the lower atmosphere, *J. Atmos. Sol.-Terr. Phys.*, **68**, 469–478, 2006.

Rishbeth, H., K. J. F. Sedgemore-Schulthess, and T. Ulich, Semiannual and annual variations in the height of the ionospheric F2-peak, *Ann. Geophys.*, **18**, 285–299, 2000.

Sethi, N. K., R. S. Dabas, and V. K. Vohra, Diurnal and seasonal variations of hmF2 deduced from digital ionosonde over New Delhi and its comparison with IRI-2001, *Ann. Geophys.*, **22**, 453–458, 2004.

Sethi, N. K., R. S. Dabas, and K. Sharma, Comparison between IRI predictions and digital ionosonde measurements of hmF2 at New Delhi during low and moderated solar activity, *J. Atmos. Sol.-Terr. Phys.*, **70**, 756–763, 2008.

Torr, M. R. and D. G. Torr, The seasonal behaviour of the F2-layer of the ionosphere, *J. Atmos. Sol.-Terr. Phys.*, **35**, 2237–2251, 1973.

Triskova, L. and J. Chum, Hysteresis in dependence of foF2 on solar indices, *Adv. Space Res.*, **18**, 145–148, 1996.

Zou, L., H. Rishbeth, I. C. F. Muller-Wodarg, A. D. Aylward, and G. H. Millward, Annual and semiannual variations in the ionospheric F2-layer, I. Modelling, *Ann. Geophys.*, **18**, 927–944, 2000.

E. Kim, J.-K. Chung, Y. H. Kim (e-mail: yhkim@cnu.ac.kr), G. Jee, S.-h. Hong, and J.-h. Cho